

# Effect of Magnetic Field on Mixed Convection Boundary Layer Flow over an Exponentially Shrinking Vertical Sheet with Suction

S. S. P. M. Isa, N. M. Arifin, R. Nazar, N. Bachok, F. M. Ali, I. Pop

**Abstract**—A theoretical study has been presented to describe the boundary layer flow and heat transfer on an exponentially shrinking sheet with a variable wall temperature and suction, in the presence of magnetic field. The governing nonlinear partial differential equations are converted into ordinary differential equations by similarity transformation, which are then solved numerically using the shooting method. Results for the skin friction coefficient, local Nusselt number, velocity profiles as well as temperature profiles are presented through graphs and tables for several sets of values of the parameters. The effects of the governing parameters on the flow and heat transfer characteristics are thoroughly examined.

**Keywords**—Exponentially shrinking sheet, magnetic field, mixed convection, suction.

## I. INTRODUCTION

THE problems of flow and heat transfer in the boundary layers of a continuous stretching/shrinking surface have attracted considerable attention of researchers due to their numerous applications in industrial manufacturing processes. Some of the applications are extraction of polymer sheets, paper production, hot rolling and glass-fiber production. Sakiadis [1], [2] first initiated the study of boundary layer flow over a stretched surface. The problems in [1] and [2] are extended to discuss the various aspects of flow and heat transfer characteristics by many researchers [3]-[5]. The effect of suction or injection on the boundary layer flow and heat transfer over a continuously stretched surface has motivated the works of Fox [6] and Chen and Char [7]. Later, Gupta and Gupta [8] emphasized that the stretching of the sheet may not necessarily be linear. The study of exponential variations of stretching velocity and temperature distributions in the flow of stretching surface has been initiated by Magyari and Keller [9]. The extended work of Magyari and Keller [9] have been reported by several researchers such as Elbashbeshy [10], Khan and Sanjayanand [11], Sanjayanand and Khan [12], Sajid and Hayat [13], and Partha et al. [14].

S. S. P. M. Isa is with the Institute for Mathematical Research, Universiti Putra Malaysia, 43400 UPM, Serdang, Selangor, Malaysia (corresponding author: phone: +603-89467939; e-mail: suzi\_isa@yahoo.com).

N. M. Arifin, N. Bachok, F. M. Ali are with the Department of Mathematics, Universiti Putra Malaysia, 43400 UPM Serdang, Selangor, Malaysia (e-mail: norihanarifin@yahoo.com).

R. Nazar is with the School of Mathematical Science, Faculty of Science and Technology, Universiti Kebangsaan Malaysia, 43600 UKM Bangi, Selangor, Malaysia (e-mail: rnm@ukm.edu.my).

I. Pop is with the Department of Mathematics, Babes-Bolyai University, R-400084 Cluj-Napoca, Romania. (e-mail: popm.ioan@yahoo.co.uk).

Recently, the boundary layer flow induced by shrinking sheet has gained considerable interest. For the shrinking sheet flow, the fluid attracted towards a slot and the vorticity generated at the shrinking sheet is not confined within a boundary layer and a steady flow is not possible unless adequate suction is applied at sheet [15]. The pioneering study of the flow due to the shrinking sheet was first observed by Miklavčič and Wang [16]. Some of the investigators focused their work on the effect of magnetic field on the boundary layer flow and heat transfer over a shrinking sheet [17]-[23]. The first attempt of studying the problem of boundary layer flow induced by an exponentially shrinking sheet was made by Bhattacharyya [24]. In the earlier study, Bhattacharyya [24] obtained the dual solutions when the mass suction parameter  $s$  satisfies the condition  $s > 2.266684$ , and consequently for  $s < 2.266684$  the flow has no solution. The work by Bhattacharyya [24] is extended by Rohni et al. [25], by adding the effect of buoyancy force. Rohni et al. [25] found that the presence of buoyancy force would contribute to the existence of triple solutions to the flow and heat transfer.

Motivated by the analyses of Rohni et al. [25], we investigate the effects of magnetic field on the flow and heat transfer characteristics of a viscous fluid over an exponentially shrinking sheet with variable temperature distribution. We employed similarity transformation to reduce the governing nonlinear boundary layer equations to nonlinear ordinary differential equations. The numerical solutions are obtained by using the shooting method. The effects of the physical parameters on the velocity profiles, temperature profiles, skin friction coefficient and local Nusselt number are analysed.

## II. MATHEMATICAL FORMULATIONS

Consider the two-dimensional incompressible, viscous and electrically conducting fluid over an exponentially permeable shrinking surface (see Fig. 1), with the effect of magnetic field. The  $x$ -axis runs along the shrinking surface in the direction opposite to the sheet motion and the  $y$ -axis is perpendicular to it. It is assumed that the surface temperature is  $T_w$  and the temperature of the fluid at infinity is  $T_\infty$ , where  $T_w > T_\infty$  corresponds to the assisting flow case (heated sheet) and the presence of opposing flow case is when  $T_w < T_\infty$  (cooled sheet). A transverse magnetic field is assumed to be applied in the  $y$ -axis. Under the assumption of Boussinesq and boundary layer approximations, the flow and heat transfer

problems are governed by the following equations:

$$\frac{\partial u}{\partial x} + \frac{\partial v}{\partial y} = 0 \tag{1}$$

$$u \frac{\partial u}{\partial x} + v \frac{\partial u}{\partial y} = \nu \frac{\partial^2 u}{\partial y^2} + g\beta(T - T_\infty) - \frac{\sigma B^2(x)}{\rho} u \tag{2}$$

$$u \frac{\partial T}{\partial x} + v \frac{\partial T}{\partial y} = \alpha \frac{\partial^2 T}{\partial y^2} \tag{3}$$

where  $u$  and  $v$  are the components of velocity in the  $x$  and  $y$  directions, respectively,  $\nu = \mu/\rho$  is the kinematic viscosity,  $\mu$  is the viscosity,  $\rho$  is the fluid density,  $g$  is the acceleration due to gravity,  $\beta$  is the thermal expansion coefficient,  $\sigma$  is the electrical conductivity,  $\alpha$  is the thermal diffusivity and  $T$  is the temperature of the fluid. In (2) we choose the special form of magnetic field  $B(x) = B_0 e^{(x/2L)}$ .

The appropriate boundary conditions are

$$\begin{aligned} \text{At } y = 0: \\ u = u_w(x) = -U_w e^{(x/L)}, \\ v = v_w(x), \\ T_w(x) = T_\infty + T_0 e^{(2x/L)} \end{aligned} \tag{4}$$

$$\begin{aligned} \text{As } y \rightarrow \infty: \\ T_w(x) = T_\infty + T_0 e^{(2x/L)}, \\ u \rightarrow 0, \\ T \rightarrow T_\infty \end{aligned}$$

where  $U_w > 0$  is the velocity of the shrinking surface and  $v_w(x) < 0$  is the wall mass suction velocity.

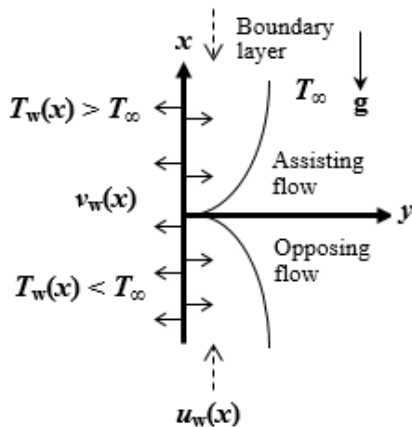


Fig. 1 Physical model and coordinate system

We introduce new similarity variables as follows:

$$\begin{aligned} \theta(\eta) &= \frac{T - T_\infty}{T_w - T_\infty}, \\ \eta &= y \left( \frac{U_w}{2\nu L} \right)^{1/2} e^{(x/2L)}, \\ u &= U_w e^{(x/L)} f'(\eta), \\ v &= - \left( \frac{U_w \nu}{2L} \right)^{1/2} e^{(x/2L)} \\ &\quad [f(\eta) + \eta f'(\eta)] \end{aligned} \tag{5}$$

By substituting (5) into (1)–(3), we obtain nonlinear ordinary differential equations:

$$f''' + ff'' - 2(f')^2 - H^2 f' + 2\lambda\theta = 0 \tag{6}$$

$$(1/\text{Pr})\theta'' + f\theta' - 4f'\theta = 0 \tag{7}$$

and (4) reduce to boundary conditions:

$$\begin{aligned} \text{At } \eta = 0: \\ f'(\eta) = -1, \\ f(\eta) = s, \\ \theta(\eta) = 1 \end{aligned} \tag{8}$$

$$\begin{aligned} \text{As } \eta \rightarrow \infty: \\ f'(\eta) \rightarrow 0, \\ \theta(\eta) \rightarrow 0 \end{aligned}$$

where  $H^2 = 2\sigma B_0^2 L / \rho U_w$  is the Hartman number,  $\text{Pr} = \nu/\alpha$  is the Prandtl number,  $s > 0$  is the suction parameter and  $\lambda = Gr/\text{Re}^2$  is the constant mixed convection parameter, where  $Gr = g\beta_T T_0 L^3 / \nu^2$  is the Grashof number and  $\text{Re} = U_w L / \nu$  is the Reynolds number. It should be noticed that  $\lambda > 0$  corresponds to assisting flow,  $\lambda < 0$  corresponds to opposing flow and  $\lambda = 0$  corresponds to forced convection flow.

The physical quantities of interest in the present problem are the skin friction coefficient  $C_f$  and the local Nusselt number  $Nu_x$ , which are given by

$$\begin{aligned} C_f &= \frac{\mu}{\rho U_w^2} \left( \frac{\partial u}{\partial y} \right)_{y=0}, \\ Nu_x &= \frac{L}{T_w - T_\infty} \left( - \frac{\partial T}{\partial y} \right)_{y=0} \end{aligned} \tag{9}$$

Substituting (5) into (9), we get

$$\begin{aligned} C_f (2\text{Re}_x)^{1/2} e^{(-3x/2L)} &= f''(0), \\ Nu_x \left( \frac{2}{\text{Re}_x} \right)^{1/2} e^{(-x/2L)} &= -\theta'(0) \end{aligned} \tag{10}$$

### III. RESULTS AND DISCUSSION

Equations (6) and (7) subject to (8) were solved numerically using the shooting method. The numerical values of the skin friction coefficient  $f''(0)$  and the local Nusselt number  $-\theta'(0)$  as well as the velocity profile  $f'(\eta)$  and temperature profile  $\theta(\eta)$  are obtained for various values of the Hartmann number  $H$ , the suction parameter  $s$ , and the mixed convection parameter  $\lambda$ . To assess the accuracy of the numerical method, we compare the present results with those obtained by Bhattacharyya [24] and Rohni et al. [25] in Table I. In this table, the comparison is made for the non-magnetic case  $H = 0$ , non-buoyant flow  $\lambda = 0$ , and when  $Pr = 1$ . This table shows the comparison for the value of the critical suction parameter  $s_c$  and singularity point of suction parameter  $s_a$ . The values of  $s_c$ , which connect the upper branch and lower branch are depicted from the graphs of the skin friction coefficient  $f''(0)$  and the local Nusselt number  $-\theta'(0)$  against  $s$ . Discontinuity points in the lower branch, which determined the singularity points are obtained from the variations of  $-\theta'(0)$  versus  $s$ . As a conclusion, the present values of  $s_c$  and  $s_a$  are in good agreement with those obtained by Bhattacharyya [24] and Rohni et al. [25]. Therefore, the good comparison gives us much confidence in our theoretical study and numerical computation. In this paper, we focus on the problem of mixed convection in the case of when the flow is opposing and assisting with the effect of magnetic field.

The effect of magnetic field and suction on the flow and heat transfer in the case of when the flow is opposing ( $\lambda < 0$ ) have been depicted in Figs. 2–5. The variation of the dimensionless skin friction coefficient  $f''(0)$  and the local Nusselt number  $-\theta'(0)$  against  $s$  when  $Pr = 1$  and  $\lambda = -0.5$  are displayed in Figs. 2 and 3. In this case, four solutions exist. The first and second solutions are combined at the critical point  $s_c$ , whereas the third solution continues until it reaches  $s = 0$  (impermeable surface). The fourth solutions occur at large values of the suction parameter  $s$ .

Next we tabulate the values of the skin friction coefficient and local Nusselt number for various values of  $s$  for  $\lambda = -0.5$  in Table II. It can be seen from Table II that larger  $H$  and  $s$  values imply higher values of  $f''(0)$  and  $-\theta'(0)$  for the first solution. The values of  $f''(0)$  and  $-\theta'(0)$  are consistently reduced by the presence of magnetic field in the second, third, and fourth solutions.

Figs. 4 and 5 show the velocity  $f'(\eta)$  and temperature  $\theta(\eta)$  profiles when  $\lambda = -1$ . From this figure, we notice that among all the profiles, the third solution has the largest magnitude of velocity, at the point of near to the shrinking wall. Then, negative velocity  $f'(\eta)$  in all profiles tend to achieve a constant value, namely zero. The temperature  $\theta(\eta)$  of fourth solution profile is initially decreasing and goes to a certain negative value, then for larger  $\eta$  the temperature starts to increase.

To study the flow and heat transfer characteristics of the assisting flow case ( $\lambda > 0$ ), we plot the skin friction coefficient  $f''(0)$  and the local Nusselt number  $-\theta'(0)$  against  $s$  when  $\lambda = 1$  in Figs. 6 and 7. Similar to the case of opposing flow, four profiles are obtained. The critical point  $s_c$  is an intersection point between the second and third solution profiles. The first and fourth solutions continue until  $s = 0$  for  $f''(0)$  and  $-\theta'(0)$ .

The values of  $f''(0)$  and  $-\theta'(0)$  for several values of  $s$  when  $\lambda = 1$  are tabulated in Table III. From Table III, it is clear that the skin friction coefficient increases with the increase of magnetic field in the first, second and third solutions. On the other hand, as  $H$  increases, the value of  $f''(0)$  decreases for the fourth solution. The values of the local Nusselt number increase with the increase of the rate of magnetic field, which is displayed in Table III. This statement is true for the first, second and fourth solutions. When we consider the third solution, the values of the local Nusselt number always decrease with increasing  $H$ . Further, Table III shows that the values of the skin friction coefficient  $f''(0)$  and the local Nusselt number  $-\theta'(0)$  increase with an increase of the rate of suction.

The graphs of the velocity profiles  $f'(\eta)$  are depicted in Fig. 8. From this figure, the velocity increases with an increase in  $\eta$  for the first solution. The velocity profiles  $f'(\eta)$  of the second and third solutions are initially decreasing at the point near to the shrinking wall. For larger value of  $\eta$ , these two solutions start to increase until they approach zero value. Fig. 9 depicts the variations on the temperature profiles. From Fig. 9, the temperature at a point for the fourth solution is found to increase initially, but it decreases for a large value of  $\eta$ . The temperature  $\theta(\eta)$  of second solution profile is decreasing near to the shrinking sheet, then the temperature starts to increase significant little away from the shrinking sheet.

The illustrations of  $f''(0)$  and  $-\theta'(0)$  versus mixed convection parameter  $\lambda$  by adding the effects of suction are shown in Figs. 10 and 11, respectively. In Fig. 10, when the convection tends to become the assisting flow case, all the profiles show the increment in the values of the skin friction coefficient. Some profiles show that the local Nusselt number increases or decreases infinitely when  $\lambda$  closes to 0. The negative values of the skin friction coefficient  $f''(0)$  show the occurrence of reverse flow; which means that there is a velocity overshoot in the boundary layer. Heat transfer from the wall to the ambient fluid is in the case of  $-\theta'(0) > 0$ , whereas reverse heat flow is indicated by  $-\theta'(0) < 0$ . From Figs 10 and 11, four solutions exist for the variations of  $f''(0)$  and  $-\theta'(0)$  in the case of  $\lambda \neq 0$ . But, dual solutions only occur when  $\lambda = 0$  in the variations of the local Nusselt number.

TABLE I  
COMPARISON OF CRITICAL SUCTION PARAMETER  $s_c$  AND SINGULARITY POINT OF SUCTION PARAMETER  $s_a$

	Parameters	
	$s_c$	$s_a$
Bhattacharyya [24]	2.266684	-
Rohni et al. [25]	2.2665	Between 2.3378 and 2.3379
Present	2.26662	Between 2.33773 and 2.33776

TABLE II  
VALUES OF SKIN FRICTION COEFFICIENT AND LOCAL NUSSELT NUMBER FOR OPPOSING FLOW CASE

$s$	$f''(0)$		$-\theta'(0)$	
	$H=0.28$	$H=0.3$	$H=0.28$	$H=0.3$
3.6	2.8475	2.8555	2.7435	2.7448
	(-1.7097)	(-1.7113)	(-5.1319)	(-5.2423)
	{-4.9553}	{-5.0030}	{1.6824}	{1.6320}
	[2.6356]	[-0.7361]	[8.8545]	[5.9416]
3.7	2.9784	2.9860	2.8794	2.8805
	(-2.0471)	(-2.0486)	(-6.1313)	(-6.2529)
	{-5.3349}	{-5.3839}	{1.7448}	{1.6940}
	[2.6580]	[-0.7320]	[9.7626]	[6.8006]
3.8	3.1064	3.1135	3.0117	3.0126
	(-2.4069)	(-2.4085)	(-7.2491)	(-7.3827)
	{-5.7441}	{-5.7943}	{1.8122}	{1.7611}
	[2.6131]	[-0.6967]	[10.7240]	[7.7951]
3.9	3.2318	3.2386	3.1411	3.1419
	(-2.7904)	(-2.7920)	(-8.4961)	(-8.6423)
	{-6.1843}	{-6.2355}	{1.8839}	{1.8327}
	[2.4624]	[-0.6166]	[11.7213]	[8.9526]
4.0	3.3551	3.3616	3.2679	3.2687
	(-3.1985)	(-3.2002)	(-9.8834)	(-10.0430)
	{-6.6569}	{-6.7088}	{1.9594}	{1.9080}
	[2.1036]	[-0.4698]	[12.6865]	[10.3084]

( ) Second solution, { } Third solution and [ ] Fourth solution

TABLE III  
VALUES OF SKIN FRICTION COEFFICIENT AND LOCAL NUSSELT NUMBER FOR ASSISTING FLOW CASE

$s$	$f''(0)$		$-\theta'(0)$	
	$H=0.28$	$H=0.3$	$H=0.28$	$H=0.3$
3.6	3.9287	3.9338	2.8980	2.8986
	(-1.2402)	(-1.2318)	(4.3046)	(4.4399)
	{-1.2077}	{-1.1308}	{2.0941}	{1.8855}
	[0.5836]	[0.2153]	[0.1568]	[0.3907]
3.7	4.0138	4.0188	3.0161	3.0166
	(-1.5867)	(-1.5796)	(5.0442)	(5.1648)
	{-1.6475}	{-1.5899}	{2.0933}	{1.9294}
	[0.6728]	[0.2564]	[-0.2097]	[-0.0199]
3.8	4.1001	4.1050	3.1334	3.1339
	(-1.9527)	(-1.9468)	(5.8033)	(5.9190)
	{-2.1323}	{-2.0892}	{2.1264}	{1.9899}
	[0.8328]	[0.3324]	[-0.6312]	[-0.3924]
3.9	4.1875	4.1923	3.2500	3.2505
	(-2.3411)	(-2.3363)	(6.6046)	(6.7198)
	{-2.6564}	{-2.6246}	{2.1764}	{2.0587}
	[1.1156]	[0.4586]	[-1.1236]	[-0.8603]
4	4.2758	4.2806	3.3659	3.3664
	(-2.7538)	(-2.7500)	2) (7.4614)	(7.5786)
	{-3.2169}	{-3.1944}	3) {2.2362}	{2.1321}
	[1.7771]	[0.6641]	4) [-1.7288]	[-1.3992]

( ) Second solution, { } Third solution and [ ] Fourth solution

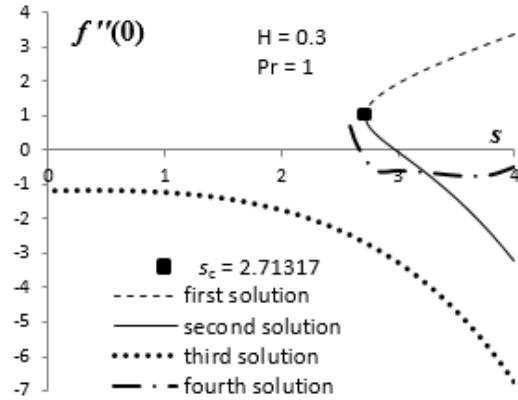


Fig. 2 Variation of  $f''(0)$  with the suction parameter  $s$  when  $\lambda = -0.5$

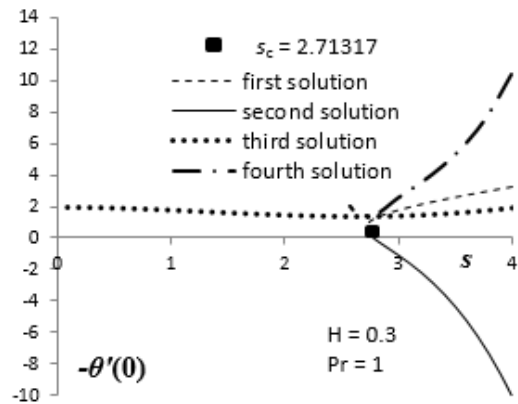


Fig. 3 Variation of  $-\theta'(0)$  with the suction parameter  $s$  when  $\lambda = -0.5$

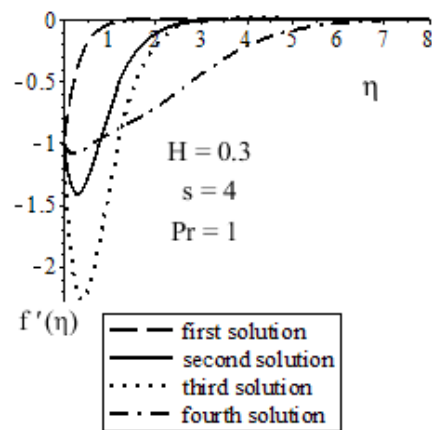


Fig. 4 Velocity profiles when  $\lambda = -1$

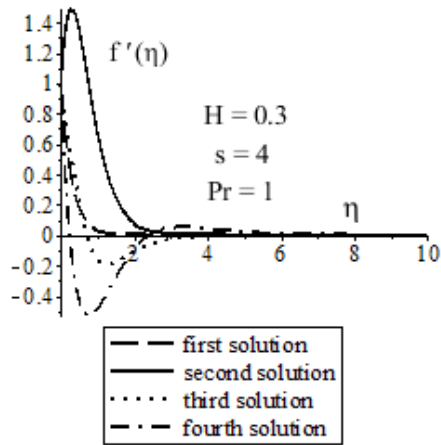


Fig. 5 Temperature profiles when  $\lambda = -1$

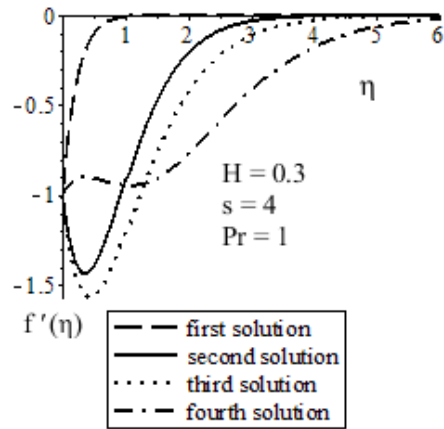


Fig. 8 Velocity profiles when  $\lambda = 1$

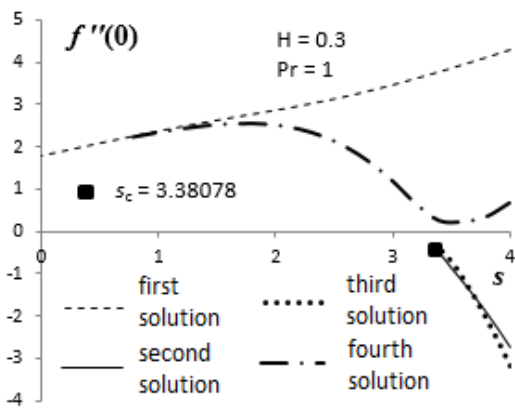


Fig. 6 Variation of  $f''(0)$  with the suction parameter  $s$  when  $\lambda = 1$

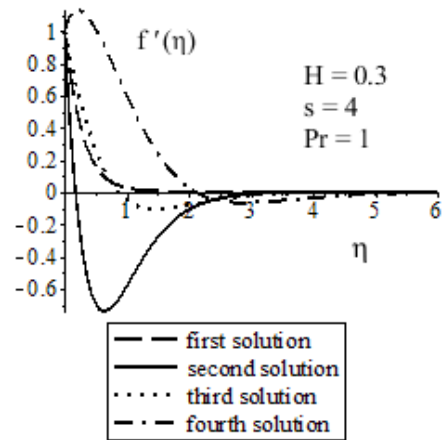


Fig. 9 Temperature profiles when  $\lambda = 1$

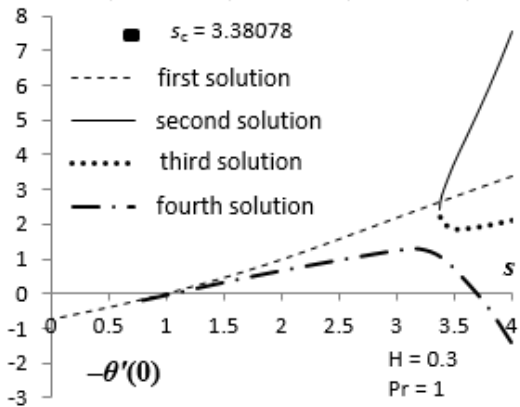


Fig. 7 Variation of  $-\theta'(0)$  with the suction parameter  $s$  when  $\lambda = 1$

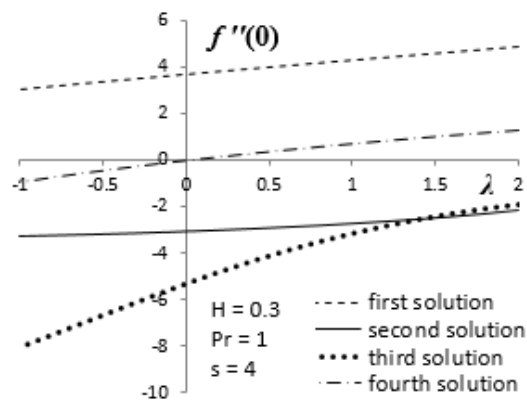


Fig. 10 Variation of  $f''(0)$  with mixed convection parameter  $\lambda$

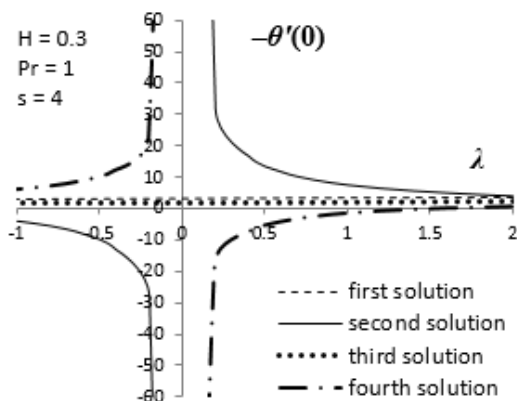


Fig. 11 Variation of  $-\theta'(0)$  with mixed convection parameter  $\lambda$

#### IV. CONCLUSION

We have studied the problem of mixed convection boundary layer flow over an exponentially shrinking sheet with suction in the presence of magnetic field. The governing partial differential equations are converted into ordinary differential equations by similarity transformation, which is then solved numerically using the shooting method. Numerical results for the skin friction and the local Nusselt number as well as the velocity and temperature profiles are shown in tables and graphs for some values of the governing parameters. Four (multiple) solutions are found for this exponentially shrinking sheet problem.

#### ACKNOWLEDGMENT

This work was supported by the research grant (FRGS) from Ministry of Education, Malaysia.

#### REFERENCES

- [1] B. C. Sakiadis, "Boundary-layer behavior on continuous solid surfaces: I. Boundary-layer equations for two-dimensional and axisymmetric flow," *AIChE J.*, vol. 7, pp. 26–28, March 1961.
- [2] B. C. Sakiadis, "Boundary-layer behavior on continuous solid surfaces: II. The boundary layer on a continuous flat surface," *AIChE J.*, vol. 7, pp. 221–225, June 1961.
- [3] F. K. Tsou, E. M. Sparrow, and R. J. Goldstein, "Flow and heat transfer in the boundary layer on a continuous moving surface," *Int J Heat Mass Transfer*, vol. 10, pp. 219–235, February 1967.
- [4] L. J. Crane, "Flow past a stretching plate," *ZAMP*, vol. 21, pp. 645–647, July 1970.
- [5] L. G. Grubka and K. M. Bobba, "Heat transfer characteristics of a continuous stretching surface with variable temperature," *Trans ASME J Heat Transfer*, vol. 107, pp. 248–250, Feb 1985.
- [6] V. G. Fox, L. E. Erickson, and L. T. Fan, "Methods for solving the boundary layer equations for moving continuous flat surfaces with suction and injection," *AIChE J.*, vol. 14, pp. 726–736, September 1968.
- [7] C. K. Chen and M. Char, "Heat Transfer over a Continuous Stretching Surface with Suction and Blowing," *J. Math. Anal. Appl.*, vol. 135, pp. 568–580, November 1988.
- [8] P. S. Gupta and A. S. Gupta, "Heat and mass transfer on a stretching sheet with suction or blowing," *Canad. J. Chem. Eng.*, vol. 55, pp. 744–746, December 1977.
- [9] E. Magyari and B. Keller, "Heat and mass transfer in the boundary layers on an exponentially stretching continuous surface," *J. Phys. D Appl. Phys.*, vol. 32, pp. 577–585, March 1999.
- [10] E. M. A. Elbashbeshy, "Heat transfer over an exponentially stretching continuous surface with suction," *Arch. Mech.*, vol. 53, pp. 643–651, May 2001.
- [11] S. K. Khan and E. Sanjayanand, "Viscoelastic boundary layer flow and heat transfer over an exponential stretching sheet," *Int. J. Heat Mass Transfer*, vol. 48, pp. 1534–1542, April 2005.
- [12] E. Sanjayanand and S. K. Khan, "On heat and mass transfer in a viscoelastic boundary layer flow over an exponentially stretching sheet," *Int. J. Therm. Sci.*, vol. 45, pp. 819–828, August 2006.
- [13] M. Sajid and T. Hayat, "Influence of thermal radiation on the boundary layer flow due to an exponentially stretching sheet," *Int. Comm. Heat Mass Transfer*, vol. 35, pp. 347–356, March 2008.
- [14] M. K. Partha, P. V. S. N. Murthy, and G. P. Rajasekhar, "Effect of viscous dissipation on the mixed convection heat transfer from an exponentially stretching surface," *Heat Mass Transfer*, vol. 41, pp. 360–366, February 2005.
- [15] T. R. Mahapatra and S. K. Nandy, "Slip effects on unsteady stagnation-point flow and heat transfer over a shrinking sheet," *Meccanica*, vol. 48, pp. 1599–1606, September 2013.
- [16] M. Miklavčič and C. Y. Wang, "Viscous flow due to a shrinking sheet," *Q. Appl. Math.*, vol. 64, pp. 283–290, April 2006.
- [17] T. Hayat, Z. Abbas, and M. Sajid, "On the analytic solution of magnetohydrodynamic flow of a second grade fluid over a shrinking sheet," *J. Appl. Mech. Trans. ASME*, vol. 74, pp. 1165–1171, Jan 2007.
- [18] T. Hayat, T. Javed, and M. Sajid, "Analytic solution for MHD rotating flow of a second grade fluid over a shrinking surface," *Phys. Lett. A*, vol. 372, pp. 3264–3273, April 2008.
- [19] T. Hayat, Z. Abbas, and N. Ali, "MHD flow and mass transfer of an upper-convected Maxwell fluid past a porous shrinking sheet with chemical reaction species," *Phys. Lett. A*, vol. 372, pp. 4698–4704, June 2008.
- [20] T. Fang and J. Zhang, "Closed-form exact solutions of MHD viscous flow over a shrinking sheet," *Commun. Nonlinear Sci. Numer. Simulat.*, vol. 14, pp. 2853–2857, July 2009.
- [21] N. F. M. Noor, S. A. Kechil, and I. Hashim, "Simple non-perturbative solution for MHD viscous flow due to a shrinking sheet," *Commun. Nonlin. Sci. Numer. Simulat.*, vol. 15, pp. 144–148, February 2010.
- [22] R. Cortell, "On a certain boundary value problem arising in shrinking sheet flows," *Appl. Math. Comput.*, vol. 217, pp. 4086–4093, December 2010.
- [23] J. H. Merkin and V. Kumaran, "The unsteady MHD boundary-layer flow on a shrinking sheet," *Eur. J. Mech. B Fluids*, vol. 29, pp. 357–363, September–October 2010.
- [24] K. Bhattacharyya, "Boundary layer flow and heat transfer over an exponentially shrinking sheet," *Chin Phys. Lett.*, vol. 28, pp. 074701-1–074701-4, April 2011.
- [25] A. M. Rohni, S. Ahmad, A. I. M. Ismail and I. Pop, "Boundary layer flow and heat transfer over an exponentially shrinking vertical sheet with suction," *Int. J. Therm. Sci.*, vol. 64, pp. 264–272, February 2013.